Stoichiometric Reductive Titrations of *Desulfovibrio gigas* Hydrogenase

Lee Melvin Roberts and Paul A. Lindahl*

Contribution from the Department of Chemistry, Texas A&M University, College Station, Texas 77843.

Received August 31, 1994®

Abstract: The NiFe hydrogenase from *Desulfovibrio gigas* contains one $[Fe_3S_4]^{1+/0}$ cluster, two $[Fe_4S_4]^{2+/1+}$ clusters, and one active-site Ni center that can be stabilized in four magnetic states (designated Ni-AB, Ni-SI, Ni-C, and Ni-R). Ni-AB and Ni-SI almost certainly correspond to Ni^{3+} and Ni^{2+} electronic states, respectively, while the electronic designations of Ni-C and Ni-R are uncertain. Ni-C arises from a species containing a photolabile hydrogenic species (H^+, H^-, or H_2). Stoichiometric reductive titrations of thionin-oxidized Hase were performed, using the reductant H_2. Titrations were monitored at 410 nm and by EPR. The resulting titration curves were simulated using two models. Each assumed that the enzyme contains the redox centers mentioned above, but they differed as to the number of electrons assumed to separate Ni-C from Ni-AB. One model assumed Ni-C was two electrons more reduced than Ni-AB, the other that it was four electrons more reduced. The former model fit the data substantially better than the latter. This restricts possible Ni-C designations to either a protonated Ni^{1+} species, a Ni^{3+} hydride, a $Ni^{3+}(n^2\text{-}H_2)$ complex, or a Ni^{2+} species with a ligand radical. An argument is expanded in support of a Ni^{1+} dithiol designation of Ni-C. Partially reduced enzyme also exhibits an unusually complex EPR signal (the $g = 2.21$ signal) that has been proposed to originate from magnetic coupling between Ni-C and one of the reduced $[Fe_4S_4]^{1+}$ clusters. The analysis presented indicates that the interacting cluster is the one with the more negative redox potential, designated Fe_{4b}. This cluster is almost certainly located nearest to the Ni center. The Ni-C/Ni-R and $[Fe_{4b}]^{2+/1+}$ couples are both in redox equilibrium with H_2. A mechanism of catalysis based on the spatial proximity and redox properties of the Ni center and Fe_{4b} is discussed.

Introduction

The NiFe hydrogenase from *Desulfovibrio gigas* (Hase[1]) catalyzes the reversible oxidation of H_2 to protons. The enzyme is an $\alpha\beta$ heterodimer that contains two $[Fe_4S_4]^{2+/1+}$ clusters, an $[Fe_3S_4]^{1+/0}$ cluster, and a mononuclear Ni complex.[2−6] Preliminary models of the X-ray crystal structure indicate that the Ni center is located in the α subunit, while the Fe−S clusters are in β.[7] The Fe−S clusters are arranged linearly, in the order $Fe_4S_4-Fe_3S_4-Fe_4S_4$. The Ni center appears to be located near one end of this arrangement, with the nearest Fe_4S_4 cluster *ca.* 13.5 Å away. The Ni center is probably the active-site, while the Fe−S clusters serve to transfer electrons between the Ni center and external redox agents.

The Ni complex can be stabilized in four states, designated **Ni-AB, Ni-SI, Ni-C,** and **Ni-R**. Ni-AB almost certainly arises from a Ni^{3+} species, and can exhibit either of two $S = {}^1/_2$ EPR signals, called Ni-A and Ni-B.[4] The EPR-silent intermediate state Ni-SI probably arises from a Ni^{2+} species. Saturation magnetization studies indicate that this Ni^{2+} state is diamagnetic.[8] Ni-C is obtained by reducing the Ni center further, and it exhibits another $S = {}^1/_2$ EPR signal indicative of either Ni^{1+} or Ni^{3+}. Ni-C is associated with a photolabile hydrogenic species (H^+, H^-, or H_2).[9−11] Ni-R is an EPR-silent state obtained by reducing Ni-C.

The electronic designations of Ni-C and Ni-R are not known with certainty and have been subject to much debate. Ni-C has been proposed to be a Ni^{3+} species,[4,12] a $Ni^{3+}-H^-$,[5] a Ni^{3+}-$(n^2\text{-}H_2)$ complex,[13] a protonated Ni^{1+} species,[6,14] a $Ni^{1+}-H^-$,[15] a $Ni^{1+}(n^2\text{-}H_2)$ complex,[16] and a Ni^{2+} species with a redox-active

* Author to whom correspondence should be addressed.

® Abstract published in *Advance ACS Abstracts,* February 1, 1995.

(1) Abbreviations: Hase, hydrogenase from *Desulfovibrio gigas*; Ni-A, the Ni center state yielding an EPR signal at $g_1 = 2.31$, $g_2 = 2.23$, $g_3 = 2.02$; Ni-B, the Ni center state yielding a signal at $g_1 = 2.33$, $g_2 = 2.16$, $g_3 = 2.02$; Ni-AB, the Ni-A and Ni-B states considered as one electronic state; Ni-SI, the EPR silent state of the Ni center more reduced than Ni-AB and more oxidized than Ni-C; Ni-C, the Ni center state yielding a signal at $g_1 = 2.19$, $g_2 = 2.16$, $g_3 = 2.02$; Ni-R the EPR-silent Ni center state that is more reduced than Ni-C; Fe_{4b}, the $[Fe_4S_4]^{2+/1+}$ cluster with the more negative potential; Fe_{4a}, the $[Fe_4S_4]^{2+/1+}$ cluster with the more positive potential; Fe_3, the $[Fe_3S_4]^{1+/0}$ cluster; A_{410}, absorbance at 410 nm; A_{min} and A_{max}, minimum and maximum absorbance at 410 nm; E_m', midpoint potential at pH 8; TED, Two-Electron-Difference Model; FED, Four-Electron-Difference Model; TED_P and FED_P, models in which only the EPR-active Ni ions are assumed redox-active; TED_T and FED_T, models in which all Ni ions in the enzyme are assumed redox-active; mnt, maleonitrile dithiolate; XAS, X-ray Absorption Spectroscopy.

(2) Moura, J. J. G.; Teixeira, M.; Moura, I.; LeGall, J. In *The Bioinorganic Chemistry of Nickel*; Lancaster, J., Ed.; VCH Publishers, New York, 1988; Chapter 9.

(3) Cammack, R.; Fernandez, V. M.; Schneider, K. In *The Bioinorganic Chemistry of Nickel*; Lancaster, J., Ed.; VCH Publishers, New York, 1988; Chapter 8.

(4) Teixeira, M.; Moura, I.; Xavier, A. V.; Huynh, B. H.; DerVartanian, D. V.; Peck, H. D.; LeGall, J.; Moura, J. J. G. *J. Biol. Chem.* **1985**, *260*, 8942−8950.

(5) Teixeira, M.; Moura, I.; Xavier, A. V.; Moura, J. J. G.; LeGall, J.; DerVartanian, D. V.; Peck, H. D.; Huynh, B. H. *J. Biol. Chem.* **1989**, *264*, 16435−16450.

(6) Cammack, R.; Patil, D. S.; Hatchikian, E. C.; Fernandez, V. M. *Biochim. Biophys. Acta* **1987**, *912*, 98−109.

(7) Volbeda, A.; Piras, C.; Charon, M. H.; Hatchikian, E. C.; Frey, M.; Fontecilla-Camps, J. C. *Int. Conf. Mol. Biol. Hydrogenases, 4th* **1994**, 146−147 (abstracts of conference held in Noordwijkerhout, The Netherlands, August 14−19, 1994).

(8) Wang, C.-P.; Franco, R.; Moura, J. J. G.; Moura, I.; Day, E. P. *J. Biol. Chem.* **1992**, *267*, 7378−7380.

(9) van der Zwaan, J. W.; Albracht, S. P. J.; Fontijn, R. D.; Slater, E. C. *FEBS Lett.* **1985**, *179*, 271−277.

(10) Fan, C.; Teixeira, M.; Moura, J. J. G.; Moura, I.; Huynh, B. H.; LeGall, J.; Peck, H. D.; Hoffman, B. M. *J. Am. Chem. Soc.* **1991**, *113*, 20−24.

(11) Whitehead, J. P.; Gurbiel, R. J.; Bagyinka, C.; Hoffman, B. M.; Maroney, M. J. *J. Am. Chem. Soc.* **1993**, *115*, 5629−5635.

(12) Kojima, N.; Fox, J. A.; Hausinger, R. P.; Daniels, L.; Orme-Johnson, W. H.; Walsh, C. *Proc. Natl. Acad. Sci. U.S.A.* **1983**, *80*, 378−382.

(13) Crabtree, R. H. *Inorg. Chim. Acta*, **1986**, *125*, L7.

0002-7863/95/1517-2565$09.00/0

ligand radical.[17] Ni-R has been proposed to be a $Ni^{2+}-H^-$,[6] a $Ni^{2+}(\eta^2-H_2)$ complex,[18] a Ni^0 species,[8] and a $Ni^{2+}(-H^-)_2$ complex.[19]

The two Fe_4S_4 clusters, designated **Fe_{4a}** and **Fe_{4b}**, have redox potentials of −290 and −340 mV *vs* NHE (at pH 7), respectively.[5] Their reduced forms exhibit broad EPR features, rather than features typical of other Fe_4S_4 clusters (namely, $g_{av} = 1.94$ signals for clusters with $S = {}^1/_2$ spin states, or features between $g = 6$ and 3 for those with $S = {}^3/_2$).[5,6,20] The Fe_3S_4 cluster, designated **Fe_3**, has a redox potential of *ca.* −70 mV, and its oxidized form exhibits an EPR signal at $g = 2.02$. All three clusters in the oxidized state absorb in the 400 nm region. A_{410} can be used to estimate the redox status of the clusters, as it declines by about 50% when the clusters become reduced.[21]

Partially-reduced Hase also exhibits a complex EPR signal, called the **$g = 2.21$** signal, thought to arise when the Ni center (in the $S = {}^1/_2$, Ni-C state) magnetically interacts with one of the reduced $[Fe_4S_4]^{1+}$ clusters.[4-6] The signal is obtained only at low temperatures and high powers, suggesting that the spin of the interacting cluster relaxes fast. Since the signal develops at potentials somewhat more negative than Ni-C, Teixeira et al. suggested that Fe_{4b} was involved.[5] However, the origin of the signal is not known with certainty.

We recently reported the first stoichiometric oxidative titration of any Hase.[21] The resulting titration curves were simulated using three model-descriptions of the redox reactions occurring in the enzyme.[22] Each model assumed three $n = 1$ Fe−S clusters, a Ni center with the four magnetic states described above, and that the Ni-C to Ni-R transition is an $n = 1$ reduction. The models differed in the number of electrons presumed to separate Ni-C from Ni-AB. The *Two-Electron-Difference* model (**TED**) assumed that Ni-C is two electrons more reduced than Ni-AB, while the *Four-Electron-Difference* model (**FED**) assumed a four electron difference, and the *Zero-Electron-Difference* model (**ZED**) assumed that Ni-C and Ni-AB are isoelectronic. Since Ni-AB almost certainly corresponds to a Ni^{3+} species, the proposed electronic designations of Ni-C can be grouped within the framework of these three models. $Ni^{3+}-H^-$, $Ni^{3+}(\eta^2-H_2)$, protonated Ni^{1+} species, and Ni^{2+} species with redox-active ligand radicals are TED-based designations, while Ni^{1+}-H^- and $Ni^{1+}(\eta^2-H_2)$ designations are FED-based, and Ni^{3+} designations are ZED-based.

The experimental titration curves fit well to TED, adequately to FED, and unsatisfactorily to ZED. The fits to ZED were so poor that the model was concluded to be incorrect. Although FED was argued to be chemically unreasonable,[22] further empirical evidence against it was required to demonstrate its incorrectness. This demonstration would limit possible electronic descriptions of Ni-C and Ni-R to those that are TED-based. These designations, in turn, impact significantly on our understanding of the catalytic mechanism.

Analyses of the oxidative titrations were also unable to discern the redox reactions occurring at very negative potentials, since the samples used were partially oxidized at the start of the titrations, and the oxidation curves of Fe_{4b}, Ni-C, and the $g = 2.21$ signals could not be observed in their entirety. These curves reflect states that are probably among the most relevant to catalysis.

In this paper, we describe the first stoichiometric reductive titrations of any Hase, and the analysis thereof. Our results provide strong evidence that Ni-C is two electrons more reduced than Ni-AB, indicating a protonated Ni^{1+}, a $Ni^{3+}-H^-$, a $Ni^{3+}(\eta^2-H_2)$ complex, or a Ni^{2+} complex with a redox-active ligand radical. They also reveal that the $g = 2.21$ signal originates from the magnetic interaction of Ni-C with $[Fe_{4b}]^{1+}$. We discuss the mechanistic implications of these results.

Experimental Procedures

Desulfovibrio gigas was grown and harvested, and Hase was purified and characterized as described.[21] Normalized intensities for the $g = 2.21$ signal were determined by measuring the signal heights of the feature at $g = 2.21$ and dividing by the maximum signal height obtained. H_2-saturated water was prepared by replacing the atmosphere above a vial of degassed water with oxygen-scrubbed (Oxisorb, MG Scientific) H_2 gas and then thoroughly mixing the solution periodically for *ca.* 90 min. The concentration of H_2 in the water (780 μM) at 25 °C was determined previously.[23]

Potentiometric titrations were performed essentially as described,[22] using two batches of Hase (1100 and 1200 units/mg of H_2 oxidation activity; >90% pure by SDS-PAGE). Anaerobically purified samples were exposed to 1 atm of H_2 for 12−16 h, then oxidized with *ca.* 6 equiv/mol of 5 mM thionin after H_2 had been chromatographically removed (Sephadex G-25). Samples were then titrated in the reductive direction using H_2-saturated water and/or H_2 gas. EPR signals were quantified using a 1 mM Cu^{2+}(EDTA) standard.[24]

Four stoichiometric reductive titrations were performed.[25] Samples were exposed to 1 atm of H_2 for 2−12 h at 30 °C, then purged 10 min with Ar and oxidized using enough 5 mM thionin to turn the samples blue. Sample 1 was freed of excess thionin by passage down a Sephadex G25 column (0.5 cm X 10 cm, equilibrated in 0.1 M potassium phosphate pH 8.0), then diluted to 2 mL with the equilibration buffer. A portion was used for EPR analysis, while the majority (1.3 mL) was used to completely fill a double-septum-sealed cuvette that contained a small quartz mixing-chip. Aliquots of H_2-saturated water were added; the solution was slowly and gently mixed by repeatedly inverting the cuvette for *ca.* 2 min. A_{410} was examined, the solution remixed, and A_{410} reexamined. This process was repeated until A_{410} was unchanged from one examination to the next. Total mixing times per aliquot ranged from 5 to 17 min. The stable A_{410} values thus obtained were assumed to reflect equilibrium conditions. The titration was terminated after adding 160 μL of H_2-saturated water, well after decreases in equilibrium A_{410} values were considered due only to dilution effects. After examination, the EPR sample was thawed anaerobically and exposed to 1 atm of H_2 overnight. The equilibrium A_{410} obtained was designated A_{min}. The sample was then exposed to air for 10 min, and the resulting equilibrium A_{410} was designated A_{max}.

The same procedure was followed for sample 2, except that the G25 column was equilibrated in 50 mM Tris pH 8.0 and the sample was diluted to 4.6 mL in that buffer. Also, a larger cuvette was used, and the solution did not fill it completely. Only 2−5 min of mixing were required to obtain stable A_{410} values. EPR spectra were not obtained.

Sample 3 was prepared similarly to sample 1, except that Schlenk techniques were used in the glovebox to minimize trace levels of H_2

(14) We use the phrase "protonated Ni^{1+} species" to indicate a Ni^{1+} complex with a protonated ligand. Complexes with protonated Ni^{1+} ions will be called Ni^{3+} hydrides.

(15) Baidya, N.; Olmstead, M. M.; Whitehead, J. P.; Bagyinka, C.; Maroney, M. J.; Mascharak, P. K. *Inorg. Chem.* **1992**, *31*, 3612−3619.

(16) Van der Zwaan, J. W.; Coremans, J. M. C. C.; Bouwens, E. C. M.; Albracht, S. P. J. *Eur. J. Biochem.* **1987**, *169*, 377−384.

(17) Bagyinka, C.; Whitehead, J. P.; Maroney, M. J. *J. Am. Chem. Soc.* **1993**, *115*, 3576−3585.

(18) Huang, Y. H.; Park, J. B.; Adams, M. W. W.; Johnson, M. K. *Inorg. Chem.* **1993**, *32*, 375−376.

(19) Surerus, K. K.; Chen, M.; van der Zwaan, J. W.; Rusnak, F. M.; Kolk, M.; Duin, E. C.; Albracht, S. P. J.; Munck, E. *Biochemistry* **1994**, *33*, 4980−4993.

(20) Fernandez, V. M; Hatchikian, E. C.; Patil, D. S.; Cammack, R. *Biochim. Biophys. Acta* **1986**, *883*, 145−154.

(21) Barondeau, D. P.; Roberts, L. M.; Lindahl, P. A. *J. Am. Chem. Soc.* **1994**, *116*, 3442−3448.

(22) Roberts, L. M.; Lindahl, P. A., *Biochemistry* **1994**, *33*, 14339−14349.

(23) Weast, R. C., Ed. *Handbook of Chemistry and Physics*, 55th ed.; CRC Press: Cleveland, 1974; B-94.

(24) Orme-Johnson, N. R.; Orme-Johnson, W. H. *Methods Enzymol.* **1978**, *52*, 252−257.

(25) Thirteen other titrations were performed but are not reported. Eight had unacceptably large scatter or were inadvertently exposed to O_2, two were incompletely characterized, one sample had low specific activity, another afforded an unidentified precipitate during the titration. The enzyme concentration obtained for another sample was unreliable. Titrations were not excluded because of incongruity with any conclusions presented.

Table 1. Determination of Enzyme Concentrations (Values in μM)

sample no.	[protein]	$[A_{max}]$	[Ni]	[Fe/11]	$[g = 2.0]_{ox}$	[av]	rel uncertainty (%)	activities (units/mg)
1	18	21	*a*	29	22	22	18	1000
2	6	9	12	9	n.d.[b]	9	22	930
3	16	17	21	22	20	19	16	1100
4	18[c], 16	22	22	25	n.d.[b]	21	19	750

[a] Value measured was not included since it was more than 10 standard deviations from the average listed. [b] Not determined. [c] Protein measured using biuret reagent.

from inadvertently reducing the sample. After the solution was diluted to 8 mL with 0.1 M potassium phosphate pH 8.0, 0.5 mL aliquots were loaded into modified EPR tubes fitted with intentionally-punctured rubber septa and quartz mixing-chips, as described.[26] Each tube was filled completely to avoid a gas phase and was injected with different volumes of H_2-saturated H_2O. Samples were repeatedly inverted for 2 min, and frozen by rapid immersion into cold hexane 5 min after H_2 was injected.

Sample 4 was prepared similarly to sample 3, except that the degree oxidized upon elution from the G25 column was determined (it was 88% oxidized). A_{max} was obtained by adding a slight excess of thionin to an aliquot and A_{min} was obtained by exposing that aliquot to H_2 for 2 h. One EPR aliquot was treated with 1.0 equiv/mol of thionin rather than H_2, to render it fully oxidized. The resulting data point was included in the EPR titration curve. The abscissa of the curve was shifted such that the resulting data point defined 0 equiv/mol.

Analysis. The resulting titration curves were simulated using the TED and FED models described previously[22] (also see Introduction). Besides three $n = 1$ redox centers (the Fe−S clusters), TED assumes that the Ni center undergoes three $n = 1$ reductions (Ni-B → Ni-SI → Ni-C → Ni-R); FED assumes that it undergoes five such reductions (Ni-B → Ni-SI → Ni-I2 → Ni-I1 → Ni-C → Ni-R). For the simulations in the reductive direction, the only significant differences in analysis were as follows: (i) H_2 and $2H^+$ replaced T_{red} and T_{ox}, respectively, in eqs 1−6 of ref 22; (ii) $E_{0(H_2)}$ replaced $E_{m(thionin)}$ and was set equal to 0 mV vs NHE at pH 0; (iii) a buffered solution at pH 8 was assumed; (iv) the two A_{410} curves from titrations 1 and 2, the two Ni-C curves from titrations 3 and 4, the Ni-B curve from titration 4, and the $g = 2.21$ titration curve from titration 4 were simultaneously simulated using the same set of E_m' values; and (v) A_{min} values for the simulations were obtained by calculating A_{410} at the H_2 concentration of H_2-saturated water. This approach was used to account for the possibility that some fraction of Fe−S clusters were not fully reduced in 1 atm of H_2. The quality-of-fit parameter, Q_{fit}, was redefined to be:

$$Q_{fit} = Q_{A_{410}(tit.\ 1)} + Q_{A_{410}(tit.\ 2)} + Q_{Ni\text{-}C(tit.\ 3)} + Q_{Ni\text{-}C(tit.\ 4)} + Q_{Ni\text{-}B(tit.\ 4)} + Q_{2.21(tit.4)}$$

The best-fit E_m values were those that yielded the lowest Q_{fit}. The number of equivalents per mol oxidized at the start-points of the four titrations differed from each other, so this parameter was allowed to vary freely for each simulation. $[Hase]_{sim}/[Hase]_{exp}$ ratios were allowed to vary freely as well, to allow for the possibility that the best-fit enzyme concentrations for each titration differed from the experimental concentration to different extents.

The $g = 2.21$ titration curve was simulated assuming that it originated from the magnetic coupling of Ni-C and either $[Fe_{4b}]^{1+}$ or $[Fe_{4a}]^{1+}$. The $g = 2.21$ relative intensity at any point in the titration was calculated to be the **product** of the concentrations of the species assumed to be involved. Thus, the $g = 2.21$ curve obtained by assuming an interaction of Ni-C and $[Fe_{4b}]^{1+}$ was given by $\{[Ni\text{-}C]\text{-}[Fe_{4b}]^{1+}\}/\{[Ni\text{-}C][Fe_{4b}]^{1+}\}_{max}$.

Chemical potentials at any point of the titrations were calculated from the Nernst equation, using calibrated best-fit E_m' values and the oxidized/reduced ratios of each redox couple. The resulting plots were averaged and smoothed. At potentials below −350 mV, the Ni-B/Ni-SI couple was unreliable and was not included in the averaging.

The titrations were analyzed using two types of TED models. TED_P (P = partial) assumes that only EPR-active Ni ions undergo redox, while TED_T (T = total) assumes that all of the Ni ions are redox-active, even those that are EPR-silent. The two types of models were required because the Ni-B EPR signal quantifies to significantly less than 1 spin/mol, and whether the EPR-silent Ni ions are redox-active is not known. The titrations were also analyzed using the FED_P model; FED_T was not used because it had been excluded previously.[22]

Results

Titrations. We performed four stoichiometric reductive titrations of thionin-oxidized Hase, using H_2 as the titrant. Table 1 lists relevant characteristics of the samples. Two titrations were monitored spectrophotometrically at 410 nm, two by EPR. The Ni-C and $g = 2.21$ signals were monitored in one EPR titration; Ni-C was monitored in the other. The Ni-C and A_{410} titration curves reflect the redox status of the Ni and Fe−S clusters, respectively. The $g = 2.21$ titration curve was presumed to reflect the interaction of Ni-C with either $[Fe_4S_4]^{1+}$ cluster.

We expected that the samples would be fully oxidized at the startpoints of the titrations, but they were actually slightly reduced (3−20% reduced at 410 nm). The reductant was probably the 10−20 ppm H_2 commonly found in our glovebox atmosphere.[21] Another possibility is that the thionin used to oxidized the samples destroyed Fe−S clusters in a few Hase molecules, releasing sulfide ions that reduced clusters in other enzyme molecules. A similar phenomenon seems to occur in carbon monoxide dehydrogenase.[27]

The two A_{410} titration curves (Figure 1, triangles) were nearly identical in shape; they declined monotonically with added H_2, curving gradually after *ca.* 4 equiv/mol of H_2 had been added. Neither curve exhibited a plateau region. This indicates that the Fe−S clusters were being reduced throughout the titration, and that at no point was only the Ni center being reduced. The end points of the titrations could not be determined visually because of the gradual curvature. This indicates that the last Fe−S cluster reduced non-stoichiometrically and was probably in redox equilibrium with H_2.

The Ni-C titration curves (Figure 2, left panel, and Figure 3, solid and open circles) developed after *ca.* 2 equiv/mol of H_2 had been added. The signal maximized at 3−4 equiv/mol, and declined thereafter. The Ni-C signals never entirely disappeared in the course of the titrations; after *ca.* 5 equiv/mol of H_2, they declined slowly. This behavior indicates that the Ni center in the Ni-C state was reduced nonstoichiometrically, and was probably in equilibrium with H_2. The $g = 2.21$ signal (Figure 2, right panel, and Figure 3, squares) developed slightly after Ni-C, maximized after *ca.* 4.5 equiv/mol of H_2, and declined thereafter.

We did not focus on the behavior of Ni-B in these titrations, since it was present in only the first few points of the titrations, and its behavior had been monitored sufficiently by the oxidative titrations[21,22] (the amount of enzyme available was also limited). The Ni-B signal was present at the startpoint of titration 1 (0.6 spin/mol), titration 3 (0.7 spin/mol), and the first two points of

(26) Shin, W.; Lindahl, P. A. *Biochemistry* **1992**, *31*, 12870−12875.

(27) Shin, W.; Stafford, P. R.; Lindahl, P. A. *Biochemistry* **1992**, *31*, 6003−6011.

(28) Van der Zwaan, J. W.; Coremans, J. M. C. C.; Bouwens, E. C. M.; Albracht, S. P. J. *Biochim. Biophys. Acta* **1990**, *1041*, 101−110.

Table 2. Best-Fit Parameters According to TED Models[a]

parameter	TED_P (Ni-C: Fe_{4b})				TED_T (Ni-C: Fe_{4b})				FED_P (Ni-C: Fe_{4b})				TED_P (Ni-C: Fe_{4a})				reported values
titration no.	1	2	3	4	1	2	3	4	1	2	3	4	1	2	3	4	
av initial equiv/mol reduced	0.30	0.39	0.37	0.01	0.33	0.45	0.28	0.01	0.40	0.40	0.39	0.00	0.48	0.35	0.31	0.02	
$[Hase]_{sim}/[Hase]_{exp}$	0.99	1.05	1.07	1.06	0.79	0.83	0.83	0.82	0.80	0.82	0.79	0.77	0.99	0.88	1.22	1.26	
E_m' ($[Fe_3]^{1+/0}$)[d]		−80				−90				−100				−110			−35,[53] −70[52]
E_m' ($[Fe_{4a}]^{2+/1+}$)[e]		−315				−320				−370				−390			−350[5,6]
E_m' ($[Fe_{4b}]^{2+/1+}$)[e]		−445				−440				−505				−445			−410[5,6]
E_m' (Ni-B/Ni-SI)[d]		−140				−140				−140				−140			140[f] −150[20]
E_m' (Ni-SI/Ni-I2)[d]		n.a.[b]				n.a.[b]				−330				n.a.[b]			n.o.[c]
E_m' (Ni-I2/Ni-I1)[d]		n.a.[b]				n.a.[b]				−330				n.a.[b]			n.o.[c]
E_m' (Ni-SI/Ni-C or Ni-I1/Ni-C)[e]		−330				−330				−330				−330			−310,[4] −390,[6] −330[22]
E_m' (Ni-C/Ni-R)[e]		−405				−400				−470				−395			−450[6]
ΔE_B		60				75				65				60			
ΔE_B		65				60				130				65			
$Q_{bestfit}/Q_{min}$		1.00				1.05				1.35				1.53			

[a] Potentials are given in mV vs NHE at or adjusted to pH 8.0. [b] Not applicable. [c] Not observed. [d] Best-fit values equals the value in the table plus ΔE_B. [e] Best-fit values equals the value in the table plus ΔE_C. [f] Present work.

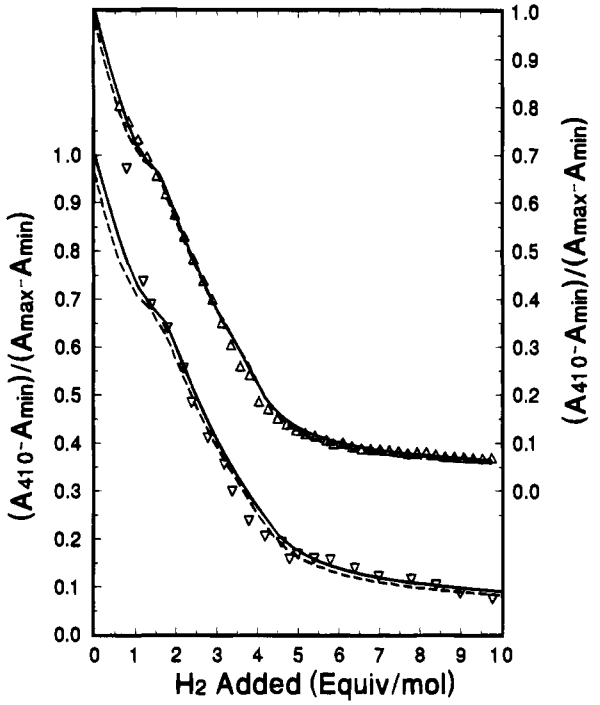

Figure 1. A_{410} curves and TED simulations for titrations 1 and 2: up triangles, titration 1; down triangles, titration 2; solid lines, best-fit TED_P simulations; dashed lines, best-fit TED_T simulations.

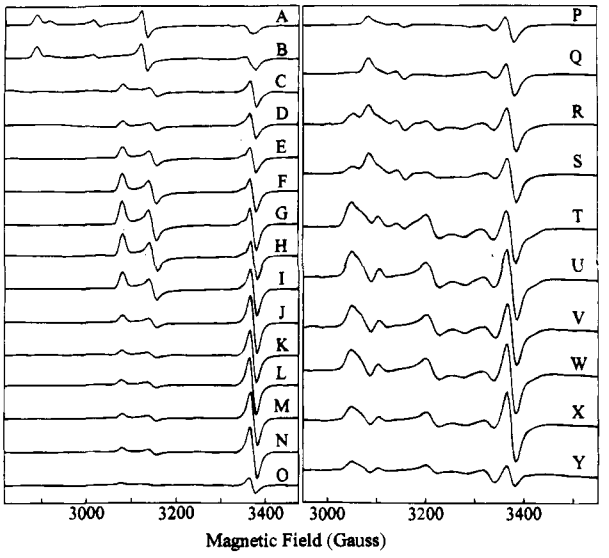

Figure 2. EPR of titration 4: A, 1.0 equiv/mol of thionin. B, directly off gel filtration column. Samples C−Y were reduced with the following number of equiv/mol of H_2: C, 1.0; D, 1.5; E, 2.0; F and P, 2.3; G and Q, 2.7; H and R, 3.0; I and S, 3.3; J and T, 3.7; K and U, 4.0; L and V, 4.3; M and W, 4.7; N and X, 5.0; O and Y, 5.6. EPR conditions for A−O: sample temperature, 100 K; microwave frequency, 9.46 GHz; microwave power, 2 mW; modulation amplitude, 11.5 G. EPR conditions for P−Y are the same, except that the sample temperature was 4.2 K, and the microwave power was 20 mW.

titration 4 (Figure 3, diamonds, 0.6 spin/mol). These low values are typical, though the reason why they are low is unknown.

Simulations. The titration curves were simulated using the TED_P, TED_T, and FED_P models, as described previously[22] and as modified in the Experimental Procedures. Sixty percent of Ni ions were assumed redox active in TED_P. The best-fit TED simulations, shown in Figures 1 and 3 (solid and dashed lines), were obtained using the parameters in Table 2. The best-fit FED_P simulations are shown in Figure 4. The shapes of the experimental curves were most faithfully reproduced by the TED_P models, as they have the lowest $Q_{best\text{-}fit}$ values (see Table 2). FED_P produced curves with shapes that fit substantially poorer to the data. The calculated FED_P best-fit A_{410} curves contained a plateau region that was absent in the data. This plateau is most severe with FED_P, because it assumes more redox chemistry at the Ni center than either TED model (redox changes in the Ni center do not change A_{410} significantly[21]).

The best-fit enzyme concentrations using TED_P differed from the experimentally determined values by 1−7% (Table 2), well within the estimated uncertainty of the experimentally determined values (average of ±19%). Those using FED_P differed from experimental values by an average of 20%, at the limit of the estimated uncertainty. Use of TED_T also yielded simulations at the limit of the estimated uncertainty.

All simulations mentioned heretofore assumed that the g = 2.21 signal originated from the magnetic interaction of Ni-C and $[Fe_{4b}]^{1+}$. This assumption yielded a best-fit simulation that was significantly better than that obtained assuming an interaction with $[Fe_{4a}]^{1+}$ (see Table 2 and compare Figure 3 to Figure 5).

Midpoint Potentials. As mentioned previously,[22] absolute E_m' values cannot be obtained from stoichiometric titrations, only differences in E_m' values among groups of redox couples with similar E_m' values. The Ni-B/Ni-SI and $[Fe_3]^{1+/0}$ couples constitute such a group. To calibrate their best-fit midpoint potentials, we measured E_m' for the Ni-B/Ni-SI couple to be −135 ± 25 mV *vs* NHE at pH 8 (Figure 6). This value was obtained in the reductive direction. E_m' for the Ni-B/Ni-SI

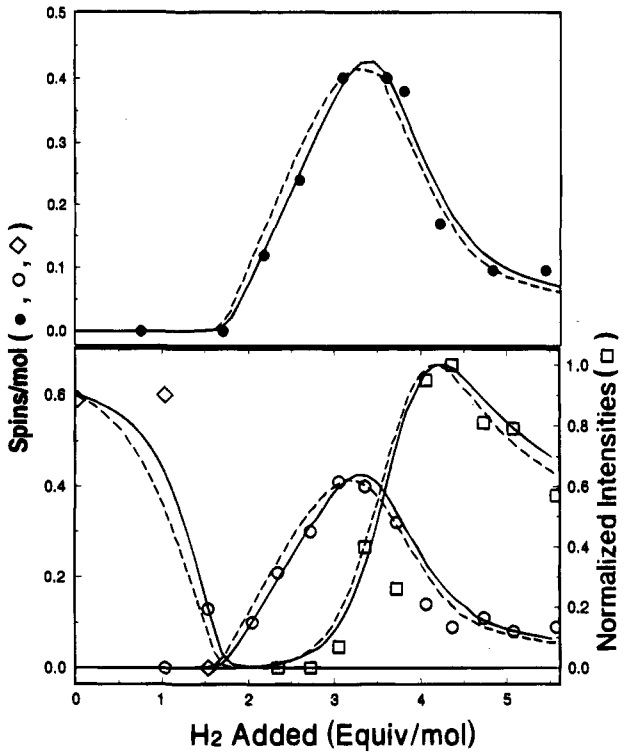

Figure 3. EPR curves and TED Simulations for titrations 3 and 4: solid circles, Ni-C curve from titration 3; open circles, Ni-C curve from titration 4; squares, $g = 2.21$ curve from titration 4; diamonds, Ni-B curve from titration 4; solid and dashed lines, simulated titration curves according to TED_P and TED_T, respectively, assuming that the $g = 2.21$ signal arises from the interaction of Ni-C and $[Fe_{4b}]^{1+}$.

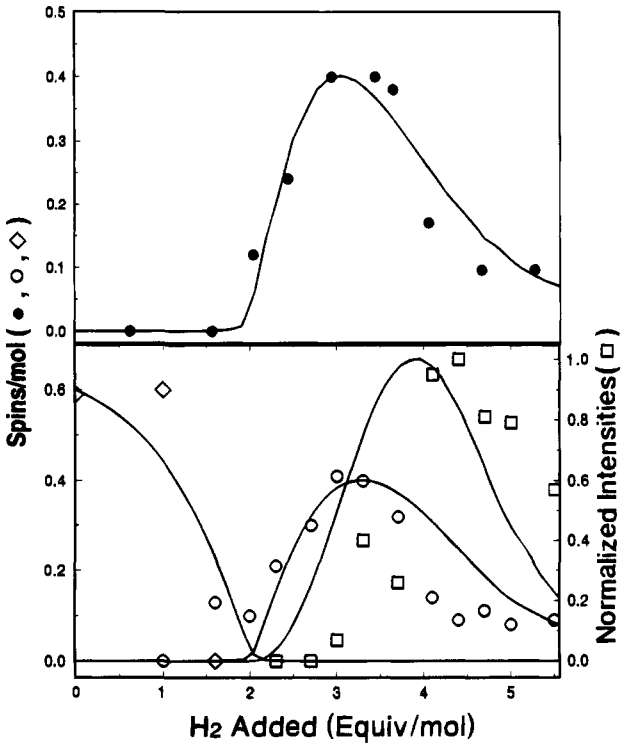

Figure 4. A_{410} and EPR curves and best-fit FED_P simulations for titrations 1–4. See Figures 1 and 3 for symbol descriptions. Lines are the best-fit FED_P simulated curves assuming that the $g = 2.21$ signal arises from the interaction of Ni-C and $[Fe_{4b}]^{1+}$.

couple was measured in the oxidative direction to be -150 ± 25 mV.[22] Thus, this couple is reversible within the uncertainties of the measurements, and the average of the midpoint potentials (-140 mV) can be regarded as a thermodynamic reduction potential. E_m' for the $[Fe_3]^{1+/0}$ cluster was adjusted using this

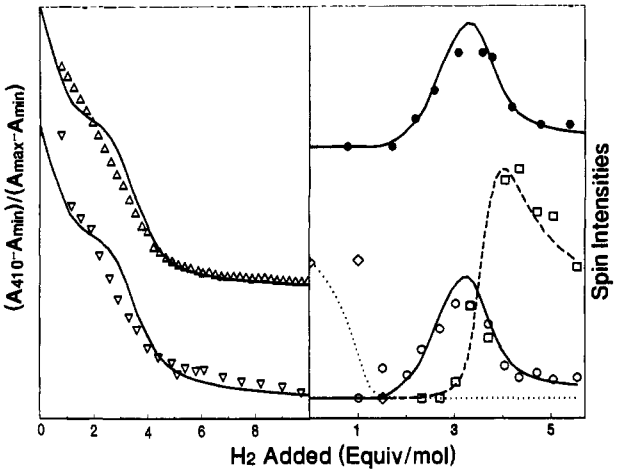

Figure 5. Best-fit TED_P simulations assuming that the $g = 2.21$ interaction signal originates from Ni-C and Fe_{4a}. See Figure 3 for symbol descriptions. Lines are the best-fit simulated titration curves according to TED_P assuming that the $g = 2.21$ signal arises from the interaction of Ni-C and $[Fe_{4a}]^{1+}$.

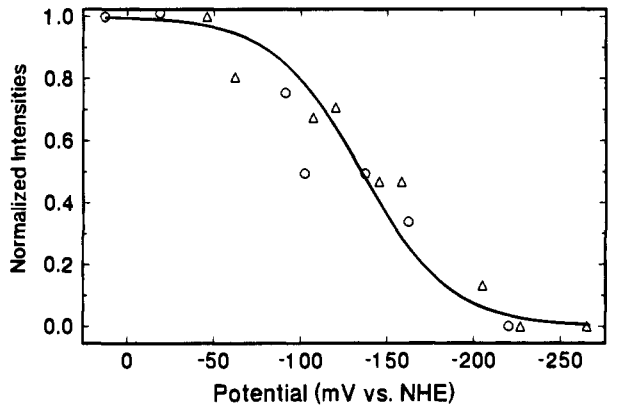

Figure 6. Potentiometric titration for the Ni-B/Ni-SI couple: triangles, sample 1 (5 points at 24 μM and 4 points at 34 μM); circles, sample 2 (19 μM). The solid line is the least-squares best-fit Nernst curve for $n = 1$, $E_m = -135$ mV vs NHE.

value, and as shown in Table 2, the best-fit calibrated value is reasonably near to its experimentally determined values.

Two other couples (Ni-SI/Ni-C and $[Fe_{4a}]^{2+/1+}$) are also stoichiometrically reduced by H_2, and their E_m' values also required calibration. We considered them as one group, since their potentials are (i) <0.1 V from each other, (ii) >0.1 V from the Ni-B/Ni-SI and $[Fe_3]^{1+/0}$ E_m' values, and (iii) significantly more positive than the Ni-C/Ni-R and $[Fe_{4b}]^{2+/1+}$ E_m' values. We assigned E_m' for the Ni-SI/Ni-C couple to the value we measured previously (-330 mV).[22] This places the $[Fe_{4a}]^{2+/1+}$ couple 20 mV from its experimentally determined value (after taking the effect of pH into account).

The proper method of calibrating the best-fit midpoint potentials for the Ni-C/Ni-R and $[Fe_{4b}]^{2+/1+}$ couples was obscured by the fact that Ni-C and $[Fe_{4b}]^{2+}$ were nonstoichiometrically reduced by H_2, and yielded titration curves that bent gradually in the vicinity of their endpoints. Since fits to such titration curves **are** sensitive to absolute E_m' values, the best-fit values for these couples (-340 and -380 mV, respectively) should have equalled those determined experimentally (-450 and -410 mV, respectively). The best-fit E_m' value for the $[Fe_{4b}]^{2+/1+}$ couple is only 30 mV from its experimentally determined value (within uncertainty), while that for the Ni-C/Ni-R couple differs by 110 mV (outside uncertainty). We do not know the reason for this large difference. However, E_m' values for the Ni-SI/Ni-C and Ni-C/Ni-R couples dictate the shape of the Ni-C curve, and our best-fit simulations require

that they differ by 75 mV. We have more confidence in this requirement than in the absolute E_m' values obtained by fitting the Ni-C curve. Thus, we calibrated the best-fit Ni-C/Ni-R couple against the experimental Ni-SI/Ni-C couple, obtaining a value of −405 mV (45 mV from its experimentally determined value).

The best-fit E_m' values for Ni-C/Ni-R and $[Fe_{4b}]^{2+/1+}$ differ by only 40 mV, and so E_m' for $[Fe_{4b}]^{2+/1+}$ can be calibrated from $E_m' = -405$ mV for Ni-C/Ni-R, affording the value −445 mV. The differences between this calibrated value (−445 mV), the best-fit value (−380 mV), and the literature value (−410 mV) probably reflect uncertainties in the calculations, measurements, and/or analysis. We report the calibrated value in Table 1, but the conclusions drawn from this analysis would not have been affected if the other values were used.

Discussion

Ni-C Is Two Electrons More Reduced Than Ni-AB. The models used to analyze the stoichiometric reductive titrations of Hase (TED_P, TED_F, and FED_P) were evaluated using three criteria, including how well the best-fit calculated titration curves simulated the shapes of the experimental curves, how near the best-fit calculated enzyme concentrations were to the experimentally determined values, and how near the calibrated best-fit midpoint potentials were to the experimentally determined values. According to these criteria, the TED_P model is outstanding. It yielded curves that had virtually the same shape as the experimental curves, using enzyme concentrations and calibrated midpoint potentials very near to those determined experimentally. In contrast, FED_P yielded curves that did not simulate the shapes of the experimental curves as well, and required enzyme concentrations and midpoint potentials that deviated substantially from experimentally determined values. The TED_T model yielded curves that simulated the shapes of the experimental curves nearly as well as TED_P, but its best-fit enzyme concentrations deviated somewhat more from experimentally determined values.

We conclude that the redox reactions occurring in Hase, within the potential range of the titrations, are those specified by the TED model: $n = 1$ reactions from one $[Fe_3S_4]^{1+/0}$ cluster and two $[Fe_4S_4]^{2+/1+}$ clusters, and three n = 1 reactions from one Ni center having four redox states (Ni-B → Ni-SI → Ni-C → Ni-R). The uncertainty in the analysis is such that one additional $n = 1$ redox center could probably be accommodated, but two such centers (or one $n = 2$ center) could not. However, our data provide no evidence for an additional $n = 1$ center.

The TED model assuming that only EPR-active Ni centers are redox-active yielded simulations that fit the data better than the model assuming all Ni centers are redox-active. This provides evidence that EPR-silent Ni centers are redox-inactive. Our oxidative titrations provided additional evidence for this.[21] Since the catalytic activity of the enzyme varies in proportion to the relative intensity of the Ni-B EPR signal,[20,28] the redox activity of the Ni center and the catalytic activity of the enzyme appear correlated. This supports the view that the Ni center is the active site, and that it functions in a reversible redox capacity during catalysis, by accepting electrons from H_2 (thereby forming protons) and donating them to protons (thereby forming H_2).

Electronic Designation of Ni-C. Since Ni-AB almost certainly arises from Ni^{3+}, these results and analyses indicate that Ni-C is either a protonated Ni^{1+} complex, a $Ni^{3+}-H^-$, a $Ni^{3+}(\eta^2-H_2)$, or a Ni^{2+} species with a redox-active ligand radical. They essentially rule out FED-based designations of Ni-C (e.g. $Ni^{1+}-H^-$ and $Ni^{1+}(\eta^2-H_2)$ complexes).

We recently argued that a Ni^{1+} dithiol designation of Ni-C and a Ni^{2+} dithiol hydride designation of Ni-R were most compatible with the established EPR, CO-binding, photochemical, and redox properties of the Ni center and related model complexes.[22] The oxidation states of the Ni were assigned as such largely because the Ni-C EPR signal has anisotropic g values (g_{xyz} = 2.19, 2.16, and 2.02) that deviate substantially from the free-electron g value (g_e), and exhibit sizable ^{61}Ni hyperfine interactions. These characteristics indicate that the unpaired electron spin resides predominantly on the Ni.[4,5,18,29] Ni^{2+}−ligand radicals exhibit g values that are more isotropic and closer to g_e.[30−32]

A different conclusion has been drawn from X-ray absorption edge studies (XAS) of the Ni center from *Thiocapsa roseopersicina* Hase, poised in various Ni states (Ni-A, Ni-B, Ni-SI, Ni-C, Ni-R, the photolyzed-Ni-C state). [The g values for the Ni signals from the Hase from *Thiocapsa roseopersicina* are nearly identical to those from the *Desulfovibrio gigas* enzyme.] Bagyinka et al. and Whitehead et al. report that the Ni X-ray absorption edge was unchanged for the different Ni states.[11,17] The edge position shifts with changes in the charge on the metal, and the charge is related to the oxidation state of the metal and covalency effects of the ligands.[33] They concluded that the Ni ion has the same oxidation state in each redox state of the Ni center (low-spin Ni^{2+}), and that one or more ligands of the Ni are redox active. Thus, the Ni-C state would be designated Ni^{2+} with a ligand radical, a designation seemingly excluded by the EPR results.

The EPR and XAS results must be reconcilable in the final analysis. The properties of the Ni-C EPR signal are certainly consistent with substantial ligand covalency.[18] Compared to the g values of the Ni-A (g_{xyz} = 2.31, 2.23, 2.02) or Ni-B (g_{xyz} = 2.33, 2.16, 2.02) signals, those of Ni-C exhibit less anisotropy and their average is closer to g_e. Moreover, the ^{61}Ni hyperfine coupling constant for Ni-C ($A \sim 20$ G for the 2.02 feature) is intermediate between that of extremely metal-based systems (A = 43 G for $[Ni^{3+}(CN)_4(OH_2)_2]^{1-}$)[34] and predominantly ligand-based systems (A = 4.5 G for $[Ni^{3+}(mnt)_2]^{1-}$).[35] They are also somewhat smaller than that reported for Ni-A.[2] Thus, the Ni-C state appears to be more covalent than Ni-A or Ni-B. The EPR analysis is entirely consistent with having the unpaired electron of Ni-C ***predominantly*** on the Ni, with ***substantial covalency*** between the Ni ion and its S ligands.

Although the XAS results may not support this view, they appear to be consistent with it. If the reduction of Ni-AB (Ni^{3+}) to Ni-C (Ni^{1+}) occurred with a change of geometry or coordination number,[36] bond length, and/or protonation state of cysteine ligands,[37] the covalency contribution to the edge position energy would likely change as well.[33,38,39] This complication regarding changes in covalency precludes a direct

(29) Salerno, J. C. In *The Bioinorganic Chemistry of Nickel*; Lancaster, J., Ed.; VCH Publishers, New York, 1988; Chapter 3.
(30) Haines, R. I.; McAuley, A. *Coord. Chem. Rev.* **1981**, *39*, 77−119.
(31) Gagné, R. R.; Ingle, D. M. *Inorg. Chem.* **1981**, *20*, 420−425.
(32) Lovecchio, F. V.; Gore, E. S.; Busch, D. H. *J. Am. Chem. Soc.* **1974**, *96*, 3109−3118.
(33) Colpas, G. J.; Maroney, M. J.; Bagyinka, C.; Kumar, M.; Willis, W. S.; Suib, S. L.; Baidya, N.; Mascharak, P. K. *Inorg. Chem.* **1991**, *30*, 920−928.
(34) Pappenhagen, T. L.; Margerum, D. W. *J. Am. Chem. Soc.* **1985**, *107*, 4576−4577.
(35) Maki, A. H.; Edelstein, N.; Davison, A.; Holm, R. H. *J. Am. Chem. Soc.* **1964**, *86*, 4580−4587.
(36) James, T. L.; Smith, D. M.; Holm, R. H. *Inorg. Chem.* **1994**, *33*, 4869−4877.
(37) Darensbourg, M. Y.; Longridge, E. M.; Payne, V.; Reibenspies, J.; Riordan, C. G.; Springs, J. J.; Calabrese, J. C. *Inorg. Chem.* **1990**, *29*, 2721−2726.
(38) Eidsness, M. K.; Sullivan, R. J.; Scott, R. A. In *The Bioinorganic Chemistry of Nickel*; Lancaster, J., Ed.; VCH Publishers, New York, 1988; Chapter 4.
(39) Furenlid, L. R.; Renner, M. W.; Szalda, D. J.; Fujita, E. *J. Am. Chem. Soc.* **1991**, *113*, 883−892.

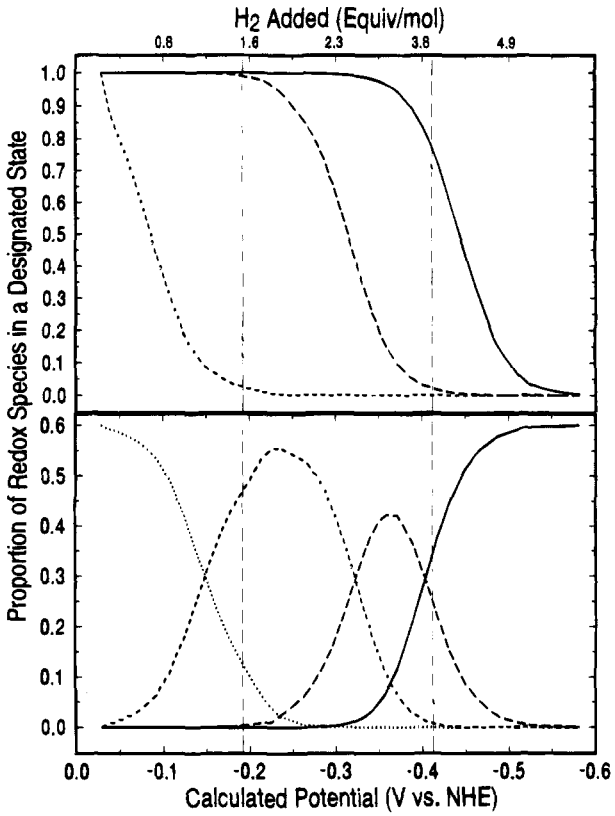

Figure 7. Decomposition of best-fit TED_P simulation of reductive titrations. Top panel: short dashed line, $[Fe_3]^{1+}$; long dashed line, $[Fe_{4a}]^{2+}$; solid line. $[Fe_{4b}]^{2+}$. Bottom panel: dotted line, Ni-B; short dashed line, Ni-SI; long dashed line, Ni-C; solid line, Ni-R. Hase has no activity at potentials to the left of the vertical line at −192 mV. Hase has H_2 oxidation activity at potentials between the two vertical lines, and proton reduction activity at potentials to the right of the vertical line at −412 mV.

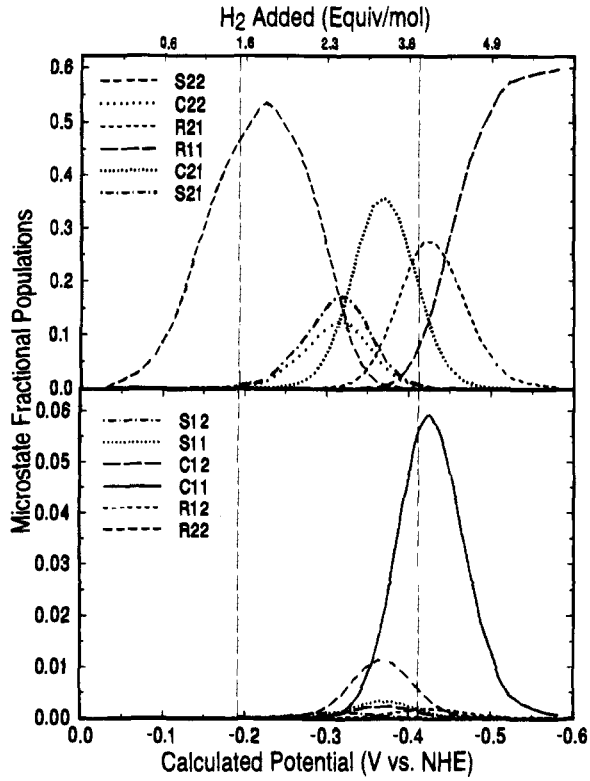

Figure 8. Redox microstates according to best-fit TED_P simulation of reductive titrations, using calibrated midpoint potentials. See text for details. Vertical lines are identical to those in Figure 7.

correlation of edge energy to Ni oxidation state.[40] Also, approximately 20% of the Ni ions in the Ni-C samples used in the XAS studies were EPR-silent (as determined using a Ni^{3+} standard rather than Cu^{2+}).[11,17,33] Our results suggest that these ions were probably in the Ni^{2+} state, and they would have further attenuated the edge changes expected for a $Ni^{2+} \rightarrow Ni^{1+}$ reduction. Taken together, these considerations render the XAS results consistent with the view that Ni-C is a Ni^{1+} complex with substantial sulfur-based covalency. Further reconciliation of the EPR and XAS results requires additional experimental studies.

Redox Microstates. We recently introduced the concept of redox microstates to provide a nomenclature that can unambiguously and conveniently specify the various combinations of redox states in Hase.[22,41] The population of a given microstate can be obtained by decomposing the simulated reductive titration curves into individual component curves (Figure 7), and then multiplying the required component curves together. For example, C12, a microstate that designates the enzyme in the Ni-C state with $[Fe_{4b}]^{1+}$ and $[Fe_{4a}]^{2+}$, is the product [Ni-C]-$[Fe_{4b}]^{1+}[Fe_{4a}]^{2+}$. The 12 microstates relevant to catalysis, obtained from the best-fit TED_P simulation, are given in Figure 8. We have not included the redox status of Fe_3 because its midpoint potential is quite high, and it appears to remain in the reduced $[Fe_3S_4]^0$ state during catalysis. Given the unusual location of this cluster between the two Fe_4S_4 clusters, it would appear to be involved in electron transfer,[7] but maybe only as a redox-inactive bridge between the two redox-active clusters.

Origin of the $g = 2.21$ Signal. Since the $g = 2.21$ signal developed in proportion to the product of [Ni-C]$^{\bullet}[Fe_{4b}]^{1+}$, not [Ni-C]$^{\bullet}[Fe_{4a}]^{1+}$, the interaction almost certainly involves Ni-C and $[Fe_{4b}]^{1+}$, the Fe_4S_4 cluster with the more negative redox potential. Since weak magnetic coupling occurs between centers separated by ~1 nm,[42] this analysis indicates that the cluster nearest the Ni center is Fe_{4b}, and the one located furthest away is Fe_{4a}.

Mechanism of Reversible Electron-Pair Splitting in NiFe Hases. The reaction catalyzed by Hases can be viewed as the reversible splitting of an electron pair (in H_2) into two single electrons (and two protons). This process appears to be facilitated by an active site that (i) is stable in three sequential redox states (Ni-SI, Ni-C, and Ni-R), (ii) has its most negative redox couple similar in potential to the H_2/H^+ couple, (iii) has the ability to change from its most oxidized to most reduced state either via one $n = 2$ reaction (Ni-SI + $H_2 \rightarrow$ Ni-R + H^+) or two $n = 1$ reactions (Ni-R $\rightarrow$ Ni-C + $e^- \rightarrow$ Ni-SI + e^-). The process also seems to require a nearby $n = 1$ redox agent ($[Fe_{4b}]^{2+/1+}$) that has a redox potential similar to the most reduced couple of the active site (Ni-C/Ni-R). Because of this arrangement, Ni-SI can oxidize H_2 (forming Ni-R), and Ni-R can rapidly reduce $[Fe_{4b}]^{2+}$ (forming Ni-C and $[Fe_{4b}]^{1+}$), thereby splitting the electron pair. If the Ni center only underwent one $n = 2$ reaction, an electron could not be transferred to the cluster. If it only underwent one $n = 1$ reaction, it could not accept the electron pair from H_2. If Fe_{4b} underwent an $n = 2$ reaction, the electron pair would not split as a result of the electron transfer. If the two centers were not near each other, the electron transfer rate would probably be slower. If the redox potentials of the couples specified above were not similar to each other

(40) Baidya, N.; Mascharak, P. K. *Trends Chem.* **1993**, *3*, 275−297.

(41) Microstates have alphanumeric designations of the form ***Nba***, where ***N*** indicates the state of the Ni (***N*** = R, C, or S corresponding to Ni-R, Ni-C, or Ni-SI, respectively), ***b*** indicates the state of Fe_{4b} (***b*** = 2 for $[Fe_{4b}]^{2+}$ and 1 for $[Fe_{4b}]^{1+}$), and ***a*** indicates the state of Fe_{4a} (***a*** = 2 for $[Fe_{4a}]^{2+}$ and 1 for $[Fe_{4a}]^{1+}$). We have not included microstates that designate Ni-B or oxidized Fe_3, since they are probably not catalytically relevant.

(42) Cammack, R.; Patil, D.; Fernandez, V. M. *Biochem. Soc. Trans.* **1985**, *13*, 572−578.

and to that of the H_2/H^+ couple, the electron-pair-splitting reaction would not occur reversibly.[43]

The other major category of hydrogenases, Fe Hases, may utilize a different mechanism. Fe-Hases contain a number of $[Fe_4S_4]^{2+/1+}$ clusters and an active-site called the *H-cluster*, but they do not contain a Ni center.[43,44] They catalyze the same reaction as the NiFe Hases, apparently by also cleaving H_2 heterolytically. H-clusters appear to be novel Fe−S clusters with six spin-coupled irons.[45,46] In their oxidized states, H-clusters are $S = {}^1/_2$ and yield EPR signals with $g_1 = 2.08$, $g_2 = 2.03$, and $g_3 = 2.00$ (for the cluster in *Clostridium pasteurianum* Hydrogenase II). The cluster can be reduced by ***one*** electron, in accordance with $E^{\circ\prime} = -410$ mV,[43] affording a diamagnetic state.[44] The H-cluster does not appear to reduce further when exposed to H_2. Thus, considering the mechanism described above, how the H-cluster reacts with H_2 and accepts an electron pair from it is puzzling, because it appears to undergo only a single $n = 1$ redox reaction. Adams has proposed a mechanism that includes a transient intermediate catalytic form of the H-cluster.[43]

Active-Reductant and Active-Oxidant Microstates. Active-reductant states of Hases are able to spontaneously reduce protons to H_2. We previously argued that R11 was the only active-reductant state of the enzyme.[22] Now that we have fairly reliable midpoint potentials for the development of Ni-R, this argument can be examined further. Plots of the enzyme's proton reduction activity as a function of chemical potential fit the Nernst equation with $n = 1$, $E_{cat}' = -420$ mV at pH 8 and have a proton dependence of 60 mV/pH[47] (right vertical dashed line, Figures 7 and 8). This potential represents the upper limit of proton reduction and the lower limit of H_2 oxidation activity (i.e. at pH 8 and potentials below −420 mV, Hase can reduce protons but cannot oxidize H_2). Although this potential does not correspond exactly to the midpoint development of any microstate, it is quite near to the potential at which R11 develops, and it has a similar pH dependence. This provides additional evidence that R11 is the active reductant state of the enzyme.

Active-oxidant states spontaneously oxidize H_2, and therefore must have the ability to accept two electrons. Since the Ni center in the Ni-R state cannot accept any electrons, R-type microstates do not appear to be active-oxidants.

The product of R11 reacting with a proton to form H_2 must be an active-oxidant state, because it is two electrons more oxidized than R11, and in redox equilibrium with H_2. According to our titrations and analysis, the only two couples in redox equilibrium with H_2 are Ni-C/Ni-R and $[Fe_{4b}]^{2+/1+}$. Thus, the resulting active-oxidant microstate would seem to correspond to C21, and in fact this microstate appears to be present after H_2 is removed from fully-reduced enzyme.[22] However, we doubt that Ni-C states are active oxidants, because Ni-C is only one electron more oxidized than Ni-R, and should therefore be incapable of accepting two electrons from H_2. S-type microstates are probably active oxidants, since they can accept two electrons. S11 would seem to be the immediate product of the reaction of R11 and a proton. According to our calibrated best-fit E_m' values, the equilibrium constant involved in converting S11 to the observed C21 state is quite large ($K = 71$), indicating that the electron transfer would readily occur.

The upper limit of H_2 oxidation occurs at *ca.* −192 mV vs NHE at pH 8 (left vertical dashed lines, Figures 7 and 8), and is thought to correspond to the reduction of Ni^{3+} to Ni^{2+}.[48] This potential corresponds roughly to the Ni-B/Ni-SI redox potential, and to the development of the S22 microstate. The correlation of this potential limit to the $Ni^{3+/2+}$ couple, as well as other experiments,[6,49,50] suggests that B-type microstates cannot react with H_2.

Mechanistic Considerations. We recently reformulated the catalytic mechanism of Cammack et al.[6] into a tricyclic form.[22] Each cycle had Ni-SI reacting with H_2 (forming Ni-R), Ni-R oxidizing in two, one-electron steps (*via* Ni-C), reforming Ni-SI, and reducing two $n = 1$ external electron acceptors. The cycles differed in the average redox status of the Fe−S clusters. Only the cycle with the most reduced clusters was proposed to operate reversibly, because only it contained the R11 active-reductant state. We proposed that reversibility was conferred on Ni-R when Fe_{4b} was reduced. With $[Fe_{4b}]^{1+}$, Ni-R (presumed to be $Ni^{2+}-H^-$) spontaneously reduces a proton to H_2, leading to proton reduction activity. With $[Fe_{4b}]^{2+}$, Ni-R preferentially reduces the cluster rather than a proton, leading to H_2 oxidation activity.

The standard free energies (at pH 8) for reactions 1 and 2

$$\text{Ni-R} + [Fe_{4b}]^{2+} = \text{Ni-C} + [Fe_{4b}]^{1+} \quad (1)$$

$$\text{Ni-R} + H^+ = \text{Ni-SI} + H_2 \quad (2)$$

are +3.8 and +21.7 KJ/mol, respectively (calculated from data in Table 2, and the relation $\Delta G^{\circ\prime} = -n\mathcal{F}\Delta E_m'$). Thus, although neither reaction occurs spontaneously (at pH 8 and under standard conditions), reducing $[Fe_{4b}]^{2+}$ is ~6 times more favorable than reducing H^+. Interestingly, H_2 oxidation activity of *Desulfovibrio gigas* Hase at pH 8 is ~6 times faster than proton reduction activity.[51] Although the relative rates of catalysis need not be related to the free energies of (1) and (2), the apparent correlation raises this possibility. Titrations and analyses similar to those reported here, using hydrogenases that catalyze proton reduction and H_2 oxidation at different relative rates, could be used to examine this possibility further.

Acknowledgment. We thank Marcetta Y. Darensbourg for helpful discussions. This work was supported by the Robert A. Welch Foundation (A-1170) and the National Institutes of Health (GM46441) and is dedicated to the memory of the late Sir Karl R. Popper.

JA9429069

(43) Adams, M. W. W. *J. Biol. Chem.* **1987**, *262*, 15054−15061.
(44) Adams, M. W. W. *Biochim. Biophys. Acta* **1990**, *1020*, 115−145.
(45) Rusnak, F. M.; Adams, M. W. W.; Mortenson, L. E.; Munck, E. *J. Biol. Chem.* **1987**, *262*, 38−41.
(46) Adams, M. W. W.; Eccleston, E.; Howard, J. B. *Proc. Natl. Acad. Sci. U.S.A.* **1989**, *86*, 4932−4936.
(47) Fernandez, V. M.; Aguirre, R.; Hatchikian, E. C. *Biochim. Biophys. Acta* **1984**, *790*, 1−7.
(48) Mege, R.-M.; Bourdillon, C. *J. Biol. Chem.* **1985**, *260*, 14701−14706.
(49) Fernandez, V. M.; Hatchikian, E. C.; Cammack, R. *Biochim. Biophys. Acta* **1985**, *832*, 69−79.
(50) Hallahan, D. L.; Fernandez, V. M.; Hatchikian, E. C.; Cammack, R. *Biochim. Biophys. Acta* **1986**, *874*, 72−75.
(51) Lissolo, T.; Pulvin, S.; Thomas, D. *J. Biol. Chem.* **1984**, *259*, 11725−11730.
(52) Teixeira, M.; Moura, I.; Xavier, A. V.; DerVartanian, D. V.; LeGall, J.; Peck, H. D.; Huynh, B. H.; Moura, J. J. G. *Eur. J. Biochem.* **1983**, *130*, 481−484.
(53) Cammack, R.; Patil, D.; Aguirre, R.; Hatchikian, E. C. *FEBS Lett.* **1982**, *142*, 289−292.